Titan's haze structure in 1999 from spatially-resolved narrowband imaging surrounding the 0.94 μm methane window

C. M. Anderson,[1] N. J. Chanover,[1] C. P. McKay,[2] P. Rannou,[3] D. A. Glenar,[4] and J. J. Hillman[5]

Received 1 March 2004; revised 29 April 2004; accepted 26 May 2004; published 23 June 2004.

[1] We use narrowband images of Titan obtained in November 1999 to explore the haze vertical structure in Titan's lower atmosphere. The images were taken with the Mount Wilson 2.54 m telescope using the NASA/GSFC-built Acousto-Optic Imaging Spectrometer. These images were recorded at five wavelengths surrounding the 0.94 μm methane window and are sensitive to a range of altitudes in Titan's lower atmosphere. We characterize Titan's limb darkening by fitting the Minnaert function limb darkening coefficient k to our data at 0° latitude and compare our observed limb darkening to that predicted from three radiative transfer models. The vertical haze profiles suggest a gap in haze below 75 km, with an increase in haze abundance near the surface. *INDEX TERMS:* 0305 Atmospheric Composition and Structure: Aerosols and particles (0345, 4801); 0343 Atmospheric Composition and Structure: Planetary atmospheres (5405, 5407, 5409, 5704, 5705, 5707); 0365 Atmospheric Composition and Structure: Troposphere—composition and chemistry; 3359 Meteorology and Atmospheric Dynamics: Radiative processes. **Citation:** Anderson, C. M., N. J. Chanover, C. P. McKay, P. Rannou, D. A. Glenar, and J. J. Hillman (2004), Titan's haze structure in 1999 from spatially-resolved narrowband imaging surrounding the 0.94 μm methane window, *Geophys. Res. Lett.*, *31*, L17S06, doi:10.1029/2004GL019857.

1. Introduction

[2] Reconnaissance of the Saturnian system by the Voyager 1 and 2 spacecraft revealed Titan, Saturn's largest moon, to be obscured by a dense, impenetrable haze [*Smith and the Voyager Imaging Science Team*, 1981]. Since the Voyager encounters, planetary scientists have relied upon ground- and space-based observations to investigate Titan's lower atmospheric structure and surface reflectivity by extending Voyager's wavelength range into the near-infrared (NIR) and imaging Titan through narrowband filters [*Smith et al.*, 1996; *Young et al.*, 2002; *Chanover et al.*, 2003]. However, we still do not know the precise haze distribution of the lower atmosphere or the composition of the surface. There is a documented north-south asymmetry that changes in brightness with season, implying that the haze distribution is dependent on the location and season on Titan [*Smith and the Voyager Imaging Science Team*, 1981; *Lorenz et al.*, 2001].

[3] The objective of this work is to investigate the transparency of the atmosphere and concentration of the haze in Titan's lower atmosphere and to further constrain the vertical aerosol distribution in Titan's lower atmosphere. The haze is directly affected by circulation patterns, condensation processes (i.e., methane or ethane rain), and photochemical processes, all of which are mechanisms that could reduce or remove the haze in the lower atmosphere. In this paper we examine the profile of the haze distribution in the lower 100 km of Titan's atmosphere and consider the extent in reduction and/or clearing of haze concentration necessary to fit our ground-based observations.

2. Observations

[4] Titan was imaged during 1999 November 03–04 with the Mount Wilson 2.54 m Hooker telescope, equipped with a natural guide star adaptive optics system. Titan's anti-Saturn hemisphere was observed, with sub-Earth longitudes of 195°W (November 3) and 220°W (November 4). At the time of the observations, the season on Titan was approaching northern winter solstice, the solar longitude L_s = 230°, and the sub-Earth latitude was 20°S. The corrected seeing for both nights was ∼0.15", resulting in five resolution elements across Titan's disk. Images were acquired with the NASA/GSFC-built Acousto-Optic Imaging Spectrometer (AImS). AImS utilizes a tunable, high spectral resolution filter element coupled to a CCD camera system and features a narrow bandpass along with spectral agility, imaging at any user-selected wavelength between 0.5–1 μm. The resolving power of this tunable filter is 3–10 times that of conventional narrowband filters. For a more detailed description of the instrument and observations, see *Chanover et al.* [2003] (hereinafter referred to as Paper I).

[5] Titan was imaged at five wavelengths centered on the 0.94 μm methane window (0.92, 0.93, 0.94, 0.95, and 0.96 μm). The November 04 images at each wavelength are shown in Figure 1. Also included in Figure 1 are North-South and East-West cuts across Titan. This data set samples a range of altitudes in Titan's lower atmosphere at a spatial resolution of ∼1100 km at the sub-Earth point. Due to the relatively large uncertainties in our absolute photometric calibration, we elected to examine the shape of Titan's absolute reflectivity curve as a function of wavelength, which is only affected by our smaller relative

[1]Department of Astronomy, New Mexico State University, Las Cruces, New Mexico, USA.
[2]Space Science Division, NASA/Ames Research Center, Moffett Field, California, USA.
[3]Service d'Aéronomie/IPSL, Université-St.-Quentin, Verrieres-le-Buisson, France.
[4]NASA/Goddard Space Flight Center, Greenbelt, Maryland, USA.
[5]Department of Astronomy, University of Maryland, College Park, Maryland, USA.

0094-8276/04/2004GL019857

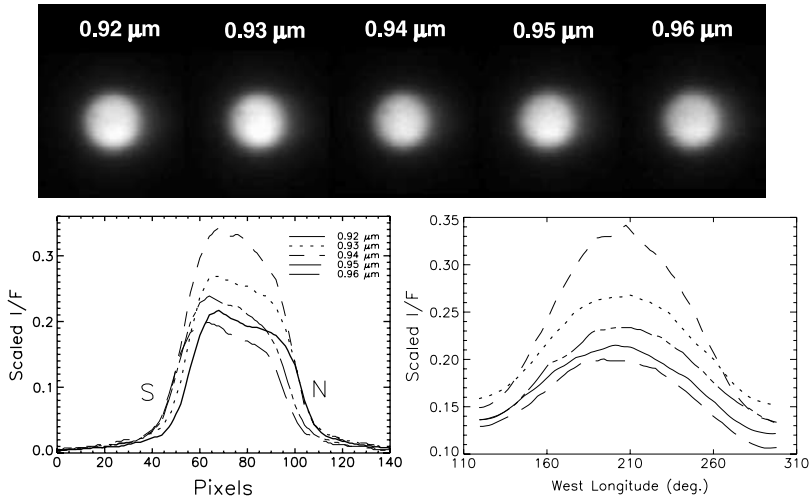

Figure 1. The images of Titan were taken on 04 November 1999 between 09:00 and 09:45 UT. The sub-Earth longitude was 220°W, which corresponds to Titan's anti-Saturn hemisphere. The plots below the Titan images are North-South (left panel) and East-West (right panel) cuts across the images for each wavelength, which samples Titan's central meridian and equator, respectively. The absolute reflectivity (I/F) has been scaled to match published geometric albedo values [*Karkoschka*, 1994].

photometry errors. Paper I contains a more thorough discussion of the image processing and data analysis.

3. Model Comparisons

[6] The wavelengths surrounding the 0.94 μm methane window are optimal for investigating the haze structure in Titan's lower atmosphere because the absorption due to methane gas is low and the haze becomes almost non-absorbing [*Khare et al.*, 1984; *McKay et al.*, 2001]. Spectral regions with minimal methane absorption, or methane windows, are not found at all wavelengths because the haze scattering extinction efficiency increases shortward of 0.94 μm [*Khare et al.*, 1984; *McKay et al.*, 2001]. Brightness variations across Titan's disk are affected by the relative importance of the surface albedo, the scattering and absorptivity of the haze, and the degree of methane absorption. At 0.94 μm, Titan's disk is limb-darkened as a result of limb geometry. In general, the limb darkening decreases longward of 0.6 μm [c.f. *Lorenz et al.*, 1997, Figure 4] because the haze becomes a less efficient scatterer.

[7] The Minnaert function $I = I_o \mu_o^k \mu^{(k-1)}$ [*Minnaert*, 1961] is an empirical relationship that characterizes the limb darkening of an object's disk, where I_o is the brightness at the center of the disk, μ_o and μ are the cosines of the incident and emergent angles of radiation, and k is the limb darkening coefficient. To interpret our Titan observations, we compared the Minnaert function limb darkening coefficient k of our observations to those predicted from three models: the one-dimensional spherical aerosol model of *McKay et al.* [1989], the one-dimensional fractal aerosol model of *Rannou et al.* [1995], and a radiative transfer model that treats the haze extinction in Titan's lower atmosphere as a free parameter, which we refer to as the free haze model. The radiative transfer models predict the total outgoing absolute reflectivity (I/F) values for eight different longitudes across Titan's disk. The *Toon et al.* [1989] radiative transfer algorithm is used to compute the I/F values. The haze production rate is disk-averaged and unable to account for latitudinal variations in haze abundance. See Paper I for a detailed description of the baseline spherical and fractal particle models.

[8] In Paper I we compared the spherical and fractal particle models to our Titan images at 0.94 μm by varying three free parameters: Titan's surface albedo between 0.1–0.3, the tropospheric methane saturation between 100%–200%, and the altitude of haze removal between 0 and 90 km. The results from Paper I suggested 100% haze removal below 80 km for the *McKay et al.* [1989] model and 100% haze removal below 50 km for the *Rannou et al.* [1995] model. Although the modeled results for the altitude of haze removal from Paper I fit our observed limb darkening data at 0.94 μm, they do not fit the wavelengths surrounding the 0.94 μm methane window.

[9] To develop a self-consistent picture of the structure of Titan's lower atmosphere, we explored the aforementioned free parameters in the spherical and fractal particle models to obtain the best fit to all the limb darkening parameters retrieved from our Titan observations at 0.92, 0.93, 0.94, 0.95, and 0.96 μm. The nightly limb darkening coefficients were averaged to obtain limb darkening at 0° latitude at each wavelength. We varied the altitude of haze removal by 10 km increments between 40 and 80 km for both the spherical and fractal particle models. For the spherical particle model, no model runs with standard input parameters [*Mckay et al.*, 1989] fit our observations at 0.93, 0.94, and 0.95 μm. We were able to fit our observations at 0.92 and 0.96 μm with an altitude of haze removal between 70 and 80 km. For the fractal particle model, we were able to fit all the wavelengths with an altitude of haze removal between 50 and 80 km.

[10] Both the spherical and fractal particle models are coupled to a microphysical model, which describes the haze properties such as particle size and density as a function of altitude [*McKay et al.*, 1989]. In the spherical particle model, particles will continue to grow until they rain out of the atmosphere (near 80 km altitude), creating a natural clearing of haze in the lower atmosphere. In contrast, fractal

particles settle slowly, introducing a haze concentration gradient in the lower atmosphere. Our multi-wavelength measurements near the 0.94 μm methane window indicate that the concentration of haze in Titan's lower atmosphere is diminished relative to the upper atmosphere [c.f. *Young et al.*, 2002], suggesting that neither of these conceptual approaches is appropriate for modeling the lower atmosphere haze profile. Rather, we use the observations themselves to constrain the haze distribution below 100 km within Titan's atmosphere.

4. Free Haze Model

[11] The free haze model treats the particles as fractals and calculates their optical properties using the method of *Rannou et al.* [1995]. Above 100 km, the haze concentration profile is constrained using Voyager observations of the upper atmospheric hazes [*Rages and Pollack*, 1983]. We used a new and improved Voyager haze profile based on a recalculation done with a more recent version of the limb inversion program (K. Rages, personal communication, 2003). The Voyager haze extinction values were scaled from 0.5 to 0.94 μm, which accounts for wavelength-dependent differences of the haze extinction coefficient. We linearly interpolated the *Khare et al.* [1984] indices of refraction of Titan tholins and applied Mie theory to appropriately scale the extinction values by the absorption efficiency factor.

[12] Below 100 km, the atmosphere was divided into four slabs: 0–25, 25–50, 50–75, and 75–100 km. Each slab was assigned an initial extinction value based on the *Young et al.* [2002] haze extinction profile. A four-parameter nonlinear least squares fitting routine, the Levenberg-Marquardt method, was used to adjust the haze extinction in the four atmospheric layers. To avoid nonphysical results within the nonlinear least squares fitting routine, the extinction values were forced to be greater than or equal to zero. The extinction values for each slab were varied until χ^2 was minimized. We use χ^2 to assess the goodness of the Levenberg-Marquardt fit between the modeled and observed Minnaert *k* coefficients.

[13] In our comparison between the observed and modeled Minnaert *k* values, we examined the surface albedo between 0.1–0.3 and the tropospheric CH_4 saturation between 100%–200%. We quantified the goodness of the fit by exploring the range in haze extinction for each model run that was within the 5% uncertainty of our observed Minnaert *k* determination. The 5% uncertainty in *k* was determined from the flat-fielding error (~2%), Poisson error (~4%), and in the uncertainty of the position of Titan's center on the images (~2%). To assess whether each model run for a given surface albedo and CH_4 supersaturation was within the 5% error, we compared the rms of the residual (R_{rms}) between the modeled and observed Minnaert values, which is proportional to χ^2. The best fit case was for surface albedo of 0.1 and a 200% methane saturated troposphere. The low surface albedo is consistent with the fact that we were observing the darker hemisphere on Titan [c.f. *Smith et al.*, 1996].

[14] A comparison between the Minnaert *k* profiles determined from the haze extinction profile of *Young et al.* [2002] and the best fit case determined from our free haze model comparison is shown in Figure 2. The best fit case Minnaert *k* profile follows the same shape as the observed Minnaert *k* values and is within the observational errors. The corresponding haze extinction values for the best fit case are depicted in Figure 3, which also shows the range in haze extinction for surface albedo of 0.1–0.3 and 100%–200% methane saturation that is within an R_{rms} less than 5%. Also shown in Figure 3 are the corresponding haze extinction profiles from the baseline spherical and fractal particle models, and the vertical haze profile from *Young et al.* [2002]. Figure 3 illustrates an inversion in haze extinction below 100 km and a drastic drop in haze extinction between 75 and 25 km. It is difficult to place lower limit constraints on the range of extinction values above 50 km since the wavelengths surrounding the 0.94 μm methane window are less sensitive to altitudes above 50 km than they are to the lower 50 km [c.f. *Young et al.*, 2002]. The total one-way haze optical depth at 0.94 μm determined with the free haze model is also given in Figure 3. Although the total optical depth of 1.53 is lower than that shown by *Young et al.* [2002], our value remains consistent with a substantial reduction/clearing of haze in the lower atmosphere.

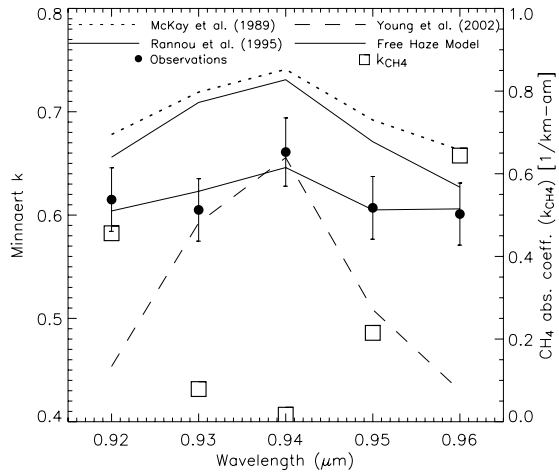

Figure 2. The best fit limb darkening *k* parameters generated from the free haze model are plotted as a function of wavelength (solid line). Superimposed are the observed Minnaert *k* values from the 1999 Titan data (filled circles) and the Minnaert *k* values derived using the haze extinction profile of *Young et al.* [2002] (dashed line). Also shown are the Minnaert *k* values derived from the baseline spherical and fractal particle models of *McKay et al.* [1989] (dotted line) and *Rannou et al.* [1995] (dot-dash line). Also shown are the methane absorption coefficients (open squares) obtained from convolving the filter transmission functions at all five wavelengths with the methane absorption spectrum of *Karkoschka* [1994].

5. Discussion

[15] Modeling the concentration of the haze and transparency of Titan's lower atmosphere with the free haze model suggests a reduction in haze concentration below 100 km, compared to previous haze extinction profiles that account for particle microphysics, which suggest an increase in haze abundance with decreasing altitude [*McKay et al.*, 1989; *Rannou et al.*, 1995]. Although the abundance

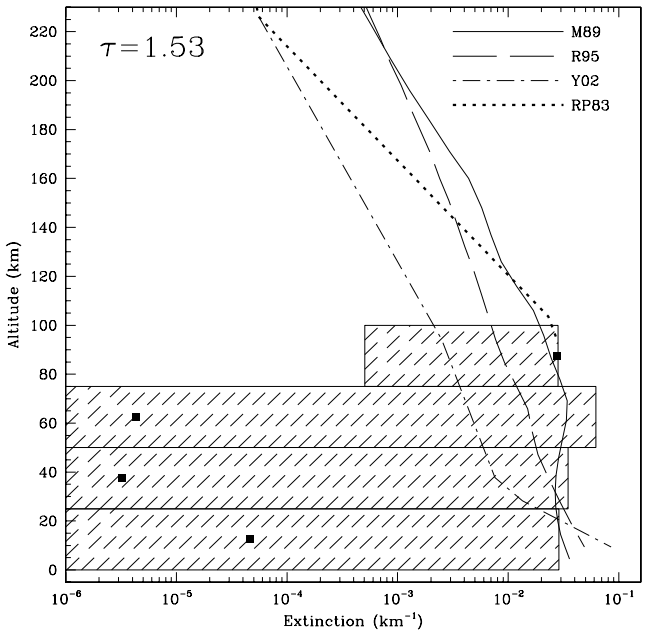

Figure 3. Haze extinction profile at 0.94 μm as a function of altitude determined from the *Rannou et al.* [1995] fractal particle model (R95, long dash line), the *McKay et al.* [1989] spherical particle model (M89, solid line), and *Young et al.* [2002] (Y02, dash-dot line). The Voyager haze extinction profile [*Rages and Pollack*, 1983] is superimposed (RP83, dotted line). The best fit case haze extinction values (filled squares) from the free haze model are superimposed, along with the range in extinction values (hatched bar regions) with an R_{rms} less than 5%. The total one-way haze optical depth (τ) of 1.53 was determined from the best fit haze extinction and will vary accordingly with the range in extinction values.

of haze at higher altitudes down to 100 km appears to be evenly mixed [*Rages and Pollack*, 1983], the trend does not continue down to the surface.

[16] The principle results of this study are:

[17] 1. The best fit case between our modeled and observed Minnaert k coefficients at all five wavelengths is for a 0.1 surface albedo and a 200% methane saturated troposphere.

[18] 2. *Rannou et al.* [2003] applied fractal haze models constrained by multiple observations to explore the haze extinction profile in the lower stratosphere and upper troposphere by simultaneously fitting the geometric albedo at 0.62 and 0.89 μm. They found that the haze extinction below 100 km must decrease down to 30 km in order to fit the albedo at 0.62 and 0.89 μm. Our results are in agreement with *Rannou et al.* [2003] regarding an extinction inversion in the lower stratosphere.

[19] 3. The haze extinction inversion continues below 75 km but steeply decreases between 75 and 25 km, with an increase in haze concentration between 25 km and the surface.

[20] A possible gap or reduction of haze below 75 km supports the conclusion from Paper 1 regarding the altitude of haze removal. Rather than a complete removal of haze below 80 or 50 km, these new results suggest a clearing of haze near those altitudes with a possibility for an increase in haze abundance near the surface. *Lorenz et al.* [1997] also found that a reduction in the haze removal altitude from 88 to 64 km could still reproduce the observed NIR contrast on Titan. The steep decrease in haze abundance between 75 and 25 km may be due to a gap in the haze, perhaps generated by some sort of clearing mechanism such as rain-out, or condensation [*Young et al.*, 2002].

[21] Another explanation for the relative clearing of haze concentration in Titan's lower atmosphere may be dynamical effects, which can be represented by eddy diffusion, a process that accelerates the vertical transport of aerosols. When the haze particles are treated as fractals, they are more readily affected by eddy diffusion because the time scale for settling of fractal particles is much longer than that of spherical aggregates. As discussed in *Rannou et al.* [2003], tropospheric condensation may not be a valid explanation for a decrease in haze extinction. Although the result of condensation may be rain-out, which decreases particle density, condensation also initiates an increase in particle size, which has little effect on altering the extent of haze extinction. A more plausible explanation for the decrease in haze extinction may be particle interaction with atmospheric dynamics, a process that cannot be fully explored using a one-dimensional representation of Titan's atmosphere.

[22] The scientific goal of the Cassini/Huygens mission at Titan is to perform a detailed study of Titan's atmosphere and to characterize the surface. Our investigation complements the Cassini/Huygens's scientific objective to study cloud physics and aerosol properties at Titan. The converse is also true, in that future remote sensing work will be closely guided by in situ measurements of the lower atmospheric haze properties by the Huygens probe.

[23] **Acknowledgments.** This work is based on observations from the Mount Wilson Observatory, which is operated by the Mount Wilson Institute under an agreement with the Carnegie Institution of Washington. Additional support was provided by the National Science Foundation under grant number AST-0074923. C.M.A acknowledges support from the Harriet G. Jenkins Predoctoral Fellowship Program, and N.J.C. acknowledges support from the Tombaugh Scholars Program. The authors thank Kathy Rages for the recalculated Voyager profile of the upper atmospheric haze extinction and two anonymous referees for their insightful comments and suggestions.

References

Chanover, N. J., C. M. Anderson, C. P. McKay et al. (2003), Probing Titan's lower atmosphere with acousto-optic tuning, *Icarus*, *163*, 150–163.

Karkoschka, E. (1994), Spectrophotometry of the Jovian planets and Titan at 300 to 1000 nm: The methane spectrum, *Icarus*, *111*, 174–192.

Khare, B. N., C. Sagan, E. T. Arakawa et al. (1984), Optical constants of organic tholins produced in a simulated Titanian atmosphere: From soft X-ray to microwave frequencies, *Icarus*, *60*, 127–137.

Lorenz, R. D., P. H. Smith, M. T. Lemmon, and E. Karkoschka (1997), Titan's north-south asymmetry from HST and Voyager imaging: Comparison with models and ground-based photometry, *Icarus*, *127*, 173–189.

Lorenz, R. D., E. F. Young, and M. T. Lemmon (2001), Titan's smile and collar: HST observations of seasonal change 1994–2000, *Geophys. Res. Lett.*, *28*, 4453–4456.

McKay, C. P., J. B. Pollack, and R. Courtin (1989), The thermal structure of Titan's atmosphere, *Icarus*, *80*, 23–53.

McKay, C. P., A. Coustenis, R. E. Samuelson et al. (2001), Physical properties of the organic aerosols and clouds on Titan, *Planet. Space Sci.*, *49*, 79–99.

Minnaert, M. (1961), Photometry of the Moon, in *Planets and Satellites*, edited by G. P. Kuiper and B. M. Middlehurst, p. 213, Univ. of Chicago Press, Ill.

Rages, K., and J. B. Pollack (1983), Vertical distribution of scattering haze in Titan's upper atmosphere, *Icarus*, *55*, 50–62.

Rannou, P., M. Cabane, E. Chassefiere et al. (1995), Titan's geometric albedo: Role of the fractal structure of the aerosols, *Icarus*, *118*, 355–372.

Rannou, P., C. P. McKay, and R. D. Lorenz (2003), A model of Titan's haze of fractal aerosols constrained by multiple observations, *Planet. Space Sci.*, *51*, 963–976.

Smith, B. A., and the Voyager Imaging Science Team (1981), Voyager 1 imaging science results, *Science*, *212*, 163–191.

Smith, P. H., M. T. Lemmon, R. D. Lorenz et al. (1996), Titan's surface, revealed by HST imaging, *Icarus*, *119*, 336–349.

Toon, O. B., C. P. McKay, T. P. Ackerman, and K. Santhanam (1989), Rapid calculation of radiative heating rates and photodissociation rates in inhomogeneous multiple scattering atmospheres, *J. Geophys. Res.*, *94*, 16,287–16,301.

Young, E. F., P. Rannou, C. P. McKay et al. (2002), A three-dimensional map of Titan's tropospheric haze distribution based on Hubble Space Telescope imaging, *Astrophys. J.*, *123*, 3473–3486.

C. M. Anderson and N. J. Chanover, Department of Astronomy, New Mexico State University, Box 30001/Dept. 4500, Las Cruces, NM 88003-0001, USA. (carrande@nmsu.edu)

D. A. Glenar, NASA/Goddard Space Flight Center, Greenbelt, MD 20771, USA.

J. J. Hillman, Department of Astronomy, University of Maryland, College Park, MD 20742, USA.

C. P. McKay, Space Science Division, Mail Stop 245-3, NASA/Ames Research Center, Moffet Field, CA 94035, USA.

P. Rannou, Service d'Aéronomie/IPSL, Université-St.-Quentin, F-91370 Verrieres-le-Buisson, France.